# Bio-geomorphological interactions in sandwave migration

B.W. Borsje
*Water Engineering and Management, University of Twente, Enschede, The Netherlands*
*Marine and Coastal Systems, Deltares, Delft, The Netherlands*

M.C. Buijsman
*Atmospheric and Oceanic Sciences, University of California, Los Angeles, USA*

G. Besio
*Civil, Environmental and Architectural Engineering, University of Genoa, Genoa, Italy*

S.J.M.H. Hulscher
*Water Engineering and Management, University of Twente, Enschede, The Netherlands*

P.M.J. Herman
*Water and Wetland Research, Radboud University, Nijmegen, The Netherlands*
*Centre for Estuarine and Marine Ecology NIOO-KNAW, Yerseke, The Netherlands*

H. Ridderinkhof
*Physical Oceanography, Royal Netherlands Institute for Sea Research, Den Burgh, The Netherlands*

ABSTRACT: Sandwave migration is observed in the Marsdiep inlet (tidal inlet between the Wadden Sea and the North Sea). Hourly measurements with an Acoustic Doppler Current Profiler (ADCP) mounted under a ferry produced high-resolution spatially explicit estimates of the rates of sandwave migration in the inlet. Physical processes responsible for the sandwave migration are different tidal components, a residual component as well as the phase difference between the tidal components. The biological community in the study area is characterized by the tube-building worms that may decelerate the near-bed flow. By including both the physical and biological processes in an idealized model, we were able (1) to reproduce the sandwave migration in the inlet and (2) to determine the contribution of the different physical and biological processes to the spatial variation in sandwave migration. The residual current is mainly responsible for the migration of sandwaves. However, for large values of the quarter-diurnal tidal component ($M_4$), sandwaves also migrate against the residual current. Biological activity can significantly influence the wavelength of sandwaves, but contribute little to the spatial variation in sandwave migration, compared to the physical processes.

## 1 INTRODUCTION

The bottom of the North Sea shows a wide variety of bedforms, among which sandwaves are the most mobile. These sandwaves originate from the interaction between tidal flow and the sandy seabed. Residual vertical circulation cells transport sediment at the bed towards the crests (Hulscher, 1996). Sandwaves have wavelengths between 100-1000 m and heights of several meters. The orientation of the crests is almost perpendicular to the direction of the main current. Field observations give an estimate of the migration of sandwaves in the Dutch part of the continental shelf of 0 m year$^{-1}$ for offshore sites up to 20 m year$^{-1}$ for coastal sites (Van Dijk and Kleinhans, 2005).

Understanding the dynamic character of the seabed is of high economic value, for example for selecting suitable locations for sandpits and windfarms (Roos and Hulscher, 2003), as well as to determine a safe burrowing depth for pipelines and telecommunication cables (Morelissen et al., 2003), and a safe navigation depth for vessels (Németh et al., 2003).

Studying the dynamics of the bottom of the seabed is not only of interest from an engineering point of view, but also from an ecological perspective. Given the high biodiversity in the subtidal area (e.g. Rabaut et al., 2007), insight is needed in the relation between geomorphodynamic processes and biota for the conservation and management of the biodiversity in the coastal zone. Moreover, benthic organisms are known to influence their habitat, resulting in bio-geomorphological interactions. Recently, Borsje et al. (2008a) showed that biota are able to influence the length of sandwaves significantly on the Belgian continental shelf. They showed that predicted sandwave lengths were closer to observations by including biological activity in an idealized model (Besio et al., 2006).

Recent studies showed that the migration of sandwaves is caused by a tidally induced residual flow (Németh et al., 2007) and higher tidal constitu-

ents (Besio et al., 2004). At the site studied in this paper, the Marsdiep inlet in the Netherlands, the migration rate of the sandwaves is up to 90 m year$^{-1}$ (Buijsman and Ridderinkhof, 2008a). This high migration rate is caused by the relatively high flow velocities in the tidal inlet, compared to the more moderate flow velocities in the offshore area studied so far.

The migration rate and wavelength of sandwaves in the Marsdiep tidal inlet show a seasonal variation, with the highest migration rate and wavelength in winter and early spring. These relatively slowly varying seasonal variations could not be explained by the abrupt occurrence of storms or estuarine circulation (Buijsman and Ridderinkhof, 2008b). Borsje et al. (2009) showed in a modeling experiment that both biological processes and physical processes could be responsible for the temporal variation in sandwave length. Physical processes responsible for the seasonal variation in sandwave length and sandwave migration rate could be the variation in tides or fall velocity of sediment particles. Moreover, biological processes show a seasonal variation, for which the decelerating of the near bottom flow by a tube building worm (*Lanice conchilega)* is characteristic for the Marsdiep tidal inlet (see next sections for more details).

However, the sandwave length and migration rate also show a spatial variation in the Marsdiep, which has not been modeled so far.

The aim of this paper is (1) to model the sandwave length and sandwave migration rate in the Marsdiep inlet and (2) to explore to what extent the spatial variability in sandwave migration rate can be caused by biological and physical processes, by varying the input parameters of an idealized sandwave model.

The structure of this paper is as follows. First the study area is introduced (Section 2), followed by a description of the idealized bio-geomorphological sandwave model (Section 3). The data obtained from an ADCP that is mounted under a ferry, which navigates between the south and north border of the study area and the model set-up is discussed subsequently (Section 4). Next, the results of the study are presented and discussed (Section 5), leading to important general conclusions (Section 6).

## 2 STUDY AREA

The study area encompasses the inlet of the Marsdiep tidal basin (52.985˚N and 4.785˚W), located in the western Dutch Wadden Sea (Figure 1). The tidal basin consists of deep tidal channels flanked by shallow sand and mud flats. The inlet is bordered by the island of Texel to the north and the town of Den Helder to the south and is about 4 km wide and maximally 27 m deep at the location where the ferry crosses. The seafloor in the inlet is covered with sand with grain sizes of 0.3-0.6 mm (Buijsman and Ridderinkhof, 2008b). The inlet is considered well-mixed and tides constitute up to 81% of the total variance of the water levels and 98% of the currents (Buijsman and Ridderinkhof, 2007). The semidiurnal tidal constituent M2 is the most dominant in the vertical and horizontal tides. The amplitude of water level variation is between 1 and 2 m. Near-surface streamwise current amplitude is between 1 and 2 m s$^{-1}$ for neap and spring tides, respectively. Currents are flood dominated in the southern half and ebb dominated in the northern half of the inlet. The bottom of the Marsdiep is inhabited by the tube building worm *Lanice conchilega* (Holtman et al., 1996). *Lanice conchilega* protrudes several centimeters from the sediment in the water column (up to 15 cm), and thereby influences the near-bottom flow. For dense tube assemblages the near-bottom flow reduces (Friedrichs et al., 2000), and consequently lower ripples are present on top of the sandwaves (Featherstone and Risk, 1977). The ripples are the main origin of bottom roughness (Soulsby, 1983). As a results the presence of *Lanice conchilega* influences the wavelength and migration rate of sandwaves in the Marsdiep inlet significantly (Borsje et al., 2009). The abundance of *Lanice conchilega* in the Marsdiep is locally extremely large (over 3,000 individuals m$^{-2}$).

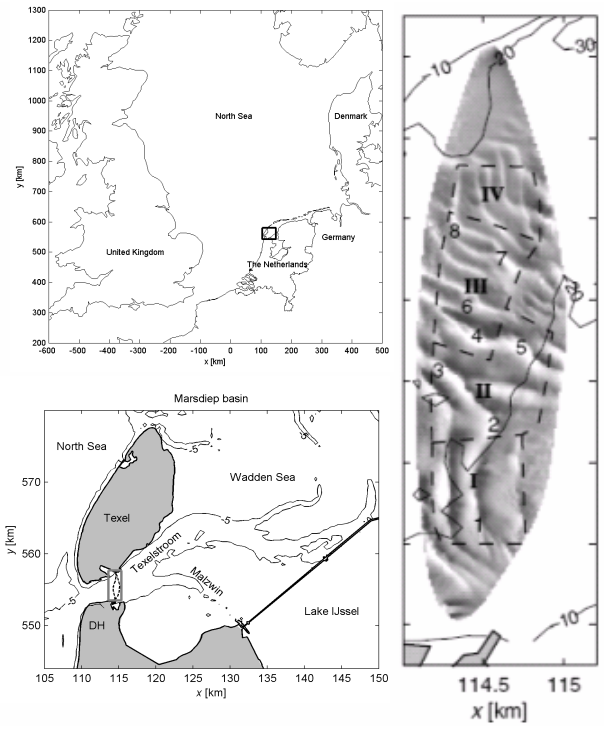


Figure 1. Overview of the study area. Sand-wave field (right), marked by the grey-lined box in the Marsdiep tidal basin (under), located in The Netherlands (top). The town of Den Helder is abbreviated with DH and the envelope of ferry crossings is indicated by the dashed line in the left plot. Dark (light) shades of grey indicate troughs (crests).

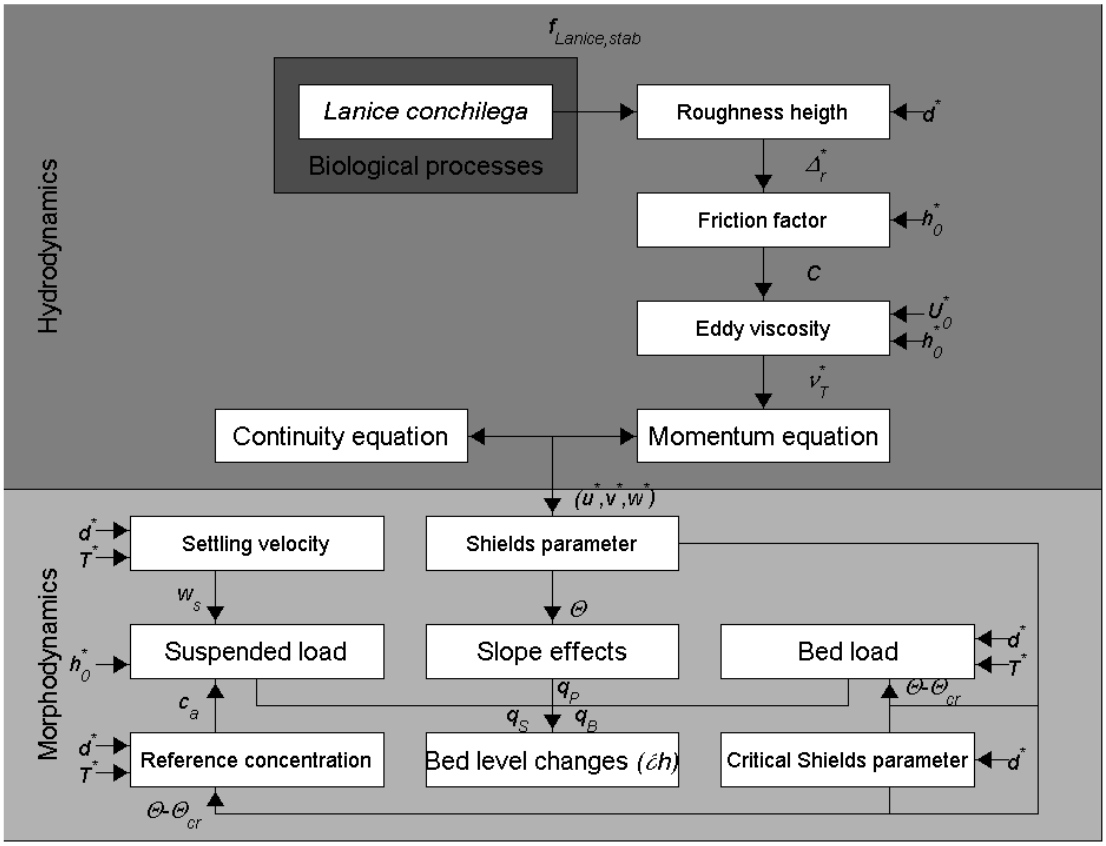


Figure 2. Model set-up, split in the hydrodynamic (Section 3.1), morphodynamic (Section 3.2) and biological part (Section 3.3). Input variables are given by the arrows in *italic* ($d^*$ = grain size, $T^*$ = Water temperature, $U^*_0$ = maximum value of the depth averaged flow velocity, $h^*_0$ = Water depth. $f_{Lanice,stab}$ = Stabilizing effect by *Lanice conchilega*) details are given in Section 3.

## 3 MODEL

To model the sandwave length and sandwave migration rate in the Marsdiep inlet we constructed an idealized bio-geomorphological model, in which sandwaves are supposed to be instabilities of the coupled system (hydrodynamics, sediment dynamics). This hypothesis was first tested by Huthnance (1982), who showed that bed patterns originate from the interaction between the sandy sea bed and the depth-averaged water motions induced by tide propagation. Hulscher (1996) elaborated on this idea by introducing a vertical flow structure, and found that sandwaves are generated by residual vertical circulation cells, whereby sediment at the bed is transported towards the crests. The hypothesis was validated for different test cases on the Dutch continental shelf (Hulscher and Van den Brink, 2001).

The hydrodynamic and morphodynamic part of the model is adopted from Besio et al. (2006), who developed a three dimensional model which is capable of predicting the main geometrical characteristics of sandwaves (wavelength, migration rate). A parameterization is added to the model to include the influence of *Lanice conchilega* on the deceleration of the near bed flow. The structure of the model is schematically shown in Figure 2. Firstly the hydrodynamics will be discussed (Section 3.1), followed by the morphodynamics (Section 3.2). The inclusion of biological activity in the model is subsequently discussed in Section 3.3.

### 3.1 *Hydrodynamics*

In the model, a shallow sea is considered with a small depth $h^*$. A Cartesian coordinate system $(x^*,y^*,z^*)$ is introduced, such that the $x^*$-axis is along the parallels pointing East, the $y^*$-axis points North along the meridian line and the $z^*$- axis is vertical pointing upward. The sea bed is supposed to be made of non-cohesive sediment of uniform size $d^*$ and density $\rho_s^*$ (a star denotes dimensional quantities).

The hydrodynamic problem is posed by continuity and momentum equations. The flow regime is assumed to be turbulent and viscous effects are neglected (a review of the characteristics of turbulence in tidal currents can be found in Soulsby, 1983).

After introducing the dimensionless variables we arrive at the following non-dimensional model:

$$\nabla \cdot \mathbf{u} = 0, \tag{1}$$

$$\frac{\partial \mathbf{u}}{\partial t} + \hat{r}\left(\mathbf{u}\cdot\nabla\right)\mathbf{u} = -\nabla p + \delta^2 \nabla\cdot\left(\upsilon_T 2\mathbf{D}\right) - \mathbf{Cor} + \mathbf{g}, \tag{2}$$

where the Boussinesq hypothesis is introduced to model the Reynolds stresses and the kinematic eddy

viscosity $\upsilon_T^*$ is written as the product of $\upsilon_{T0}^* \upsilon_T$. The constant $\upsilon_{T0}^*$ is dimensional and provides the order of magnitude of the eddy viscosity, while $\upsilon_T = \upsilon_T(x,y,z,t)$ is a dimensionless function (of order 1) describing the spatial and temporal variations of the turbulence structure, $p$ is the pressure, **D** is the strain rate tensor, $\boldsymbol{u} = (u,v,w)$ is the velocity vector. Moreover **Cor** represents the Coriolis effects and **g** is the dimensionless gravity acceleration. In (2) two dimensionless parameters appear which read:

$$\hat{r} = \frac{U_0^*}{h_0^* \sigma^*}; \; \delta = \frac{\sqrt{\upsilon_{T0}^* / \sigma^*}}{h_0^*}. \tag{3a,b}$$

Here, the parameter $\hat{r}$ is the ratio between the length of the tidal excursion and the local water depth ($\sigma$ is the angular frequency of the tide). The parameter $\delta$ represents the ratio between the thickness of the viscous bottom boundary layer generated by the tidal wave and the local water depth. The maximum value $U_0^*$ of the depth averaged fluid velocity during the tidal cycle is used as velocity scale.

The hydrodynamic problem is closed by forcing appropriate boundary conditions and providing the function $\upsilon_T^*$. Details on the boundary conditions can be found in Besio et al., (2006). The eddy viscosity $\upsilon_T^*$ is assumed to depend on the distance from the bed:

$$\upsilon_T^* = k \frac{U_0^* h_0^*}{C} F(\zeta). \tag{4}$$

The function $F(\zeta)$ ($\zeta = z^*/h^*$) describes the vertical structure of the eddy viscosity and is chosen as suggested by Dean (1974), such that the eddy viscosity grows linearly with the distance from the bed, when a region close to the bed is considered, and then decreases achieving a finite small value at the free surface. Further, in (8), $k$ is the von Karman constant ($k$=0.41) and $C$ is the friction factor, defined by:

$$C = 5.75 \log \frac{10.9 h_0^*}{z_r^*}, \tag{5}$$

where $z_r^*$ is the roughness size related to the height of the ripples, which are present on top of the sandwaves and are the main origin of the sea bed roughness (Soulsby, 1983). To calculate the height of the ripples $\Delta_r^*$, the empirical predictor is used:

$$\Delta_r^* = 202 d^* R_p^{-0.369}, \tag{6}$$

where $R_p$ is the Reynolds number of sediment particles:

$$R_p = \frac{\sqrt{\left(\rho_s^* / \rho^* - 1\right) g^* d^{*3}}}{\nu^*}, \tag{7}$$

where $\upsilon^*$ is the kinematic viscosity of water ($\upsilon^* = 1.10^{-6}$ m$^2$ s$^{-1}$ for water of 20 °C). Then, following the suggestion of Van Rijn (1991), $z_r^*$ is fixed equal to $\Delta_r^*$.

### 3.2 *Sediment transport*

In the model, sediment transport is split in two components. The first component is the bed load transport, which is the sediment moving close to the bed. Secondly, the suspended load transport is the sediment transported in suspension. The bed load transport is corrected for the fact that sediment is transported more easily downhill than uphill (slope effects). The dimensionless bed load transport $(q_{Bx}, q_{By})$ is modeled according to the relationship proposed by Van Rijn (1991):

$$(q_{Bx}, q_{By}) = \frac{0.25}{R_p^{0.2}} \left( \frac{\vec{\theta} - \theta_{cr}}{\theta_{cr}} \right)^{1.5} \left( \frac{\theta_x, \theta_y}{\sqrt{\vec{\theta}}} \right) \mathrm{H}\left( 1 - \frac{\theta_{cr}}{\theta_x, \theta_y} \right). \tag{8}$$

The Heaviside function H is equal to zero for negative arguments and is equal to 1 for positive arguments. In (8), $\theta_{cr}$ is the critical Shields parameter below which no sediment moves. $\vec{\theta}$ is equal to $\sqrt{(\theta_x^2 + \theta_y^2)}$, and the Shield parameter in x- and y- component are:

$$\left(\theta_x, \theta_y\right) = \frac{\left(\tau_x^*, \tau_y^*\right)}{\left(\rho_s^* - \rho^*\right) g^* d^*}, \tag{9}$$

where $(\tau_x^*, \tau_y^*)$ are the shear stress components, which can easily be evaluated by means of the constitutive law. The correction of the bed load transport for the variation in bed topography $(q_{Px}, q_{Py})$ is related to the dimensionless bed load transport and the local bed slope.

The dimensionless suspended load transport $(q_{Sx}, q_{Sy})$ is calculated by using a standard convection-diffusion equation for the dimensionless sediment concentration $c(x,y,z,t)$. Two boundary conditions impose the dimensionless suspended sediment concentrations at the bed and at the free surface. The latter states the vanishing of sediment flux normal to the free surface, while the former forces a reference concentration $c_a$ at a distance equal to 0.01 $h$ from the seabed. Following Van Rijn (1991):

$$c_a = 1.5 \frac{d}{R_p^{0.2}} \left( \frac{\vec{\theta} - \theta_{cr}}{\vec{\theta}} \right)^{3/2}, \tag{10}$$

where $d$ is the dimensionless grain size $d = d^*/h_0^*$. The dimensionless suspended load transport is computed as the flux of concentration over the water column, and the total dimensionless sediment transport $(q_{Tx}, q_{Ty})$ is:

$$(q_{Tx}, q_{Ty}) = (q_{Bx}, q_{By}) + (q_{Px}, q_{Py}) + (q_{Sx}, q_{Sy}). \tag{11}$$

Bed level changes can be calculated by a sediment continuity equation, which in dimensionless form is:

$$\frac{\partial h}{\partial T} = \frac{\partial q_{Tx}}{\partial x} + \frac{\partial q_{Ty}}{\partial y}. \quad (12)$$

Relation (12) simply states that convergence (or divergence) of the sediment flux must be accompanied by a rise (or fall) of the bed profile.

### 3.3 *Biological processes*

To model the influence of *L. conchilega* on the near bottom flow, we represent the tube building worm by thin vertical cylinders on the bottom of the seabed. In this way, we are able to include the worms in a vegetation model (Uittenbogaard, 2003). This vegetation model is able to calculate the turbulent flow over and through vegetation (thin columns) in water of limited depth. The vegetation model explicitly accounts for the influence of cylindrical structures on drag and turbulence by an extra source term of friction force in the momentum equation and an extra source term of Total Kinetic Energy (TKE) and turbulent energy dissipation in the $k$-$\varepsilon$ equations respectively. The vegetation model is included in Delft3D-FLOW model, which is a three-dimensional hydrodynamic model. The Delft3D-FLOW model computes flow characteristics (flow velocity, turbulence) dynamically in time over a three-dimensional spatial grid. For a detailed mathematical description of the vegetation model see Bouma et al. (2007).

Validation of the model outcome is done by Borsje et al. (2008b). The flow deceleration by *L. conchilega* will reduce the ripple height both directly and indirectly, as observed in the field by Featherstone and Risk (1977). Directly, by a decrease in energy near the bed and indirectly due to deposition of fine particles in the tube fields and consequently lower ripples. Moreover, another indirect effect is the increase in density of the benthic community with the presence of *L. conchilega* (Rabaut et al., 2007). These bio-engineers burrow and crawl through the top layer of the sediment and in this way break down the ripples. Reduction of the ripple height in the field is site specific (local sediment sorting, amount of suspended sediment and abundance of burrowing and crawling species), and therefore difficult to express in general terms. However, following the empirical relations derived by O'Donoghue et al. (2006), the ripple height will reduce to 60%, given a reduction of the near bottom flow to 30% of the original near bottom flow velocity. A reduction of 70% of the bottom flow is chosen to represent the maximum density of *L. conchilega* found in the North Sea area (Borsje et al., 2008c). Assuming a break down of the ripples by 10% due to the burrowing and crawling of the bio-engineers, the maximum reduction of the ripple height is 70%: ($f_{Lanince,stab}$ = 0.3)

$$\Delta_r^{bio} = \Delta_r^0 f_{Lanice,stab}, \quad (13)$$

where $f_{Lanince,stab}$ is the stabilizing biological factor for the ripple height. The superscript '0' for the ripple height represent the values without the influence of biological activity (default).

To calculate the migration rate of sandwaves, the Bio-geomorphological model needs 5 different input variables: waterdepth, grain size, water temperature, destabilizing factor by *Lanice conchilega* and the flow velocity (Figure 2). The flow velocity needs to be split in several components: the $M_2$ tidal component, the $M_4$ tidal component and the $Z_0$ residual current need to be prescribed. Finally, the phase difference between the $M_2$ and $M_4$ tidal component needs to be prescribed.

## 4 DATA AND MODELING SET-UP

For the investigation of the seasonal variation in sandwave length and migration rate, we use ADCP velocity data from 1999 to the end of 2002. The methodology to analyze the current data is presented in Buijsman and Ridderinkhof (2007). The ADCP was mounted under the ferry Schulpengat at 4.3 m below the water surface and recorded eastward velocities u, northward velocities v, and upward velocities w in bins of 0.5 m. The ferry crosses the inlet every half hour up to 32 times per day. Similar to Buijsman and Ridderinkhof (2008b), time gaps in the time series were filled with harmonic fits.

In addition to velocities, the ADCP also measured water depth. As is extensively discussed in Buijsman and Ridderinkhof (2008a), for the period 1998-2005 water depths collected during 30-d periods were corrected for offsets and assembled in bathymetric maps (digital elevation models; DEMs) with a grid size of 15x15 $m^2$. An example of a DEM is presented in Figure 1. From these DEMs sand-wave height H* and wavelength L* were extracted. Moreover, the sand-wave migration rate ($U_w^*, V_w^*$) was obtained by spatially correlating patterns on DEMs that were about three months apart. In this paper we use $U_{ws}^*$, which is the migration rate along the main axes of ($U_w^*, V_w^*$).

The range in values for the $M_2$ tidal component, $M_4$ tidal component, $Z_0$ residual flow and the phase difference between the M2 and M4 tidal component are given in Table 1, as well as parameter settings for a representative location in the Marsdiep inlet (Area II; Figure 1).

Table 1. Typical parameter settings for the Marsdiep inlet (Area II).

| Parameter | unit | Mean | Min | Max |
|---|---|---|---|---|
| Waterdepth | [m] | 20 | - | - |
| Grain size | [mm] | 0.4 | - | - |
| Water temperature | [°C] | 10 | - | - |
| Stabilizing factor | [-] | 0.5 | 0.25 | 0.75 |
| $M_2$ tidal component | [m $s^{-1}$] | 0.9 | - | - |
| $M_4$ tidal component | [m $s^{-1}$] | 0.09 | 0.075 | 0.13 |
| $Z_o$ residual flow | [m $s^{-1}$] | 0.04 | -0.15 | 0.05 |
| Phase difference $M_2/M_4$ | [°] | 75 | 45 | 102 |

## 5 RESULTS AND DISCUSSION

For the mean parameter setting from Table 1, the modeled wavelength is around 250 m. This value is comparable to the measured wavelength of around 200 m at this location (Area II). The wavelength of the sandwaves is hardly dependent on the combination of tidal constituents, showing that the $M_2$ tidal component has the largest contribution to the wavelength of the sandwaves. However, the migration rate of the sandwaves is greatly dependent on the different combinations of the tidal forcing.

For the given settings of the tidal forcing, the $Z_0$ component has a positive impact on the migration rate and the $M_4$ component has a negative impact on the migration rate.

Given a measured migration rate of around 60 m $year^{-1}$ we can conclude the model is able to represent both the wavelength and migration rate of the sandwaves in the Marsdiep inlet.

Borsje et al. (2009) already discussed that seasonal variability in biological processes are not the main determinant in seasonal variability in sandwave migration rate. Give the results of the model (figure 4) we can conclude that biological processes are not the main determinant in sandwave migration, given the influence of the residual current and the M4 tidal component.

The results of the model show that the residual current is the main determinant for sandwave migration rate in the Marsdiep inlet. The direction of migration is almost perfectly related to the direction of the residual current. However, for some parameter settings (phi > 60° and $M_4 > 0$) sandwaves also migrate against the residual current. Compared to field measurements, the sandwave migration in the southern part of the tidal inlet is predicted well (sandwaves migrate to the east). However, in the Northern part of the inlet, sandwaves migrate against the residual current, which is only partly captured by the model.

Buijsman and Ridderinkhof (2008b) already discussed that migration against the residual current can be caused by the suspended sediment gradient found between the North Sea and the Wadden Sea.

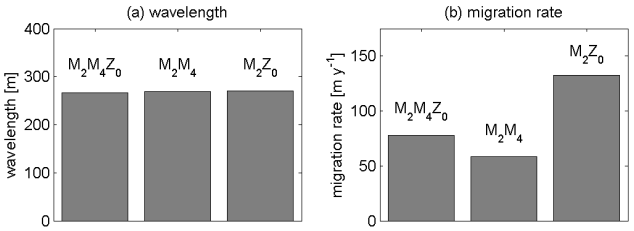


Figure 3. Modeled wavelength (a) and migration rate (b). For different combinations of the tidal forcing (mean parameter setting).

While this model computes a suspended sediment profile at one location, a gradient in suspended sediment concentration cannot be included in the model. As a result, the model is not able to predict the migration rate in the North part of the inlet. However, for the Southern part of the inlet, the model is capable to predict the spatial variation in sandwave migration rate.

The stabilizing factor by biota is based on an assumed biomass variation of *Lanice conchilega* in the Marsdiep inlet, combined with the parameterization proposed by Borsje et al. (2008b). To ground the assumed biomass variation in the Marsdiep inlet, field experiments and video camera experiments are planned to be executed in the study area.

## 6 CONCLUSION

This paper examines whether biological and physical processes are capable of causing the spatial variation in migration rate of sandwaves in the Marsdiep inlet (The Netherlands).

As model input the measured variation in tidal components is used and an assumption on the biomass variation of the tube building worm *Lanice conchilega* is included in the bio-geomorphological model. *Lanice conchilega* is known for the decelerating of the near bottom flow and in this way decrease the ripple height on top of the sandwaves.

The migration rate in the Southern part of the inlet is reproduced by the bio-geomorphological model. However, the migration of the sandwaves in the Northern part of the inlet against the residual current is only partly reproduced by the model. Possible explanation for the discrepancy is the dominance of suspension transport over bedload transport in the Northern part of the inlet. The gradient in suspended sediment transport cannot be included in the model, while the model is a 1DV model. The extension of the model to include the gradient in suspended sediment transport will be an important challenge for future. Moreover, field experiments on the biomass variation in the Marsdiep inlet are planned to ground the assumptions made in this study.

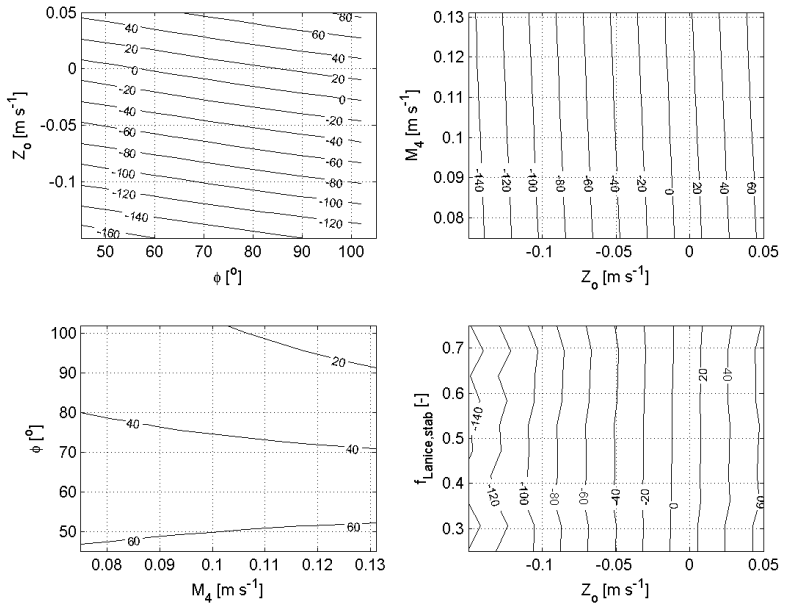


Figure 4. Sensitivity in the migration rate (m year$^{-1}$), for different combinations of the residual current ($Z_0$), $M_4$ tidal component and phase difference between $M_2$ and $M_4$ tidal component. Positive migration rates indicate migration to the east (Figure 1). Mean parameter settings are given in Table 1.

## REFERENCES


Besio, G., Blondeaux, P. Brocchini, M., Vittori, G., 2004. On the modeling of sandwave migration. Journal of Geophysical Research 109. doi 10.1029/2002JC001622.

Besio, G., Blondeaux, P., Vittori, G., 2006. On the formation of sandwaves and sand banks. Journal of Fluid Mechanics 557, 1-27.

Borsje, B.W., Besio, G., Blondeaux, P., Hulscher, S.J.M.H., Vittori, G., 2008a. Exploring biological influence on offshore sandwave length. Marine and River Dune Dynamic III, International Workshop, April 1-3 2008, Leeds. Parsons D.R., Garlan T., Best J.L. (Eds), pp 31-38.

Borsje, B.W., Hulscher, S.J.M.H., Herman, P.M.J., de Vries, M.B., 2008b. On the parameterization of biological influences on offshore sandwave dynamics. Proceedings PECS 2008, Liverpool.

Borsje, B.W., Bouma, T.J., De Vries, M.B., Hulscher, S.J.M.H., Herman, P.J., Besio, G., 2008c. Bio-geomorphological interactions in offshore seabed patterns. 31st International Conference on Coastal Engineering (ICCE), Hamburg.

Borsje, B.W., Buijsman, M.C., Besio, G., De Vries, M.B., Hulscher, S.J.M.H., Herman, P.M.J., Ridderinkhof, H., 2009. Modelling biophysical influences on sandwave dynamics. In: Proceedings of the NCK-days 2009, Texel, The Netherlands, pp. 30.

Bouma, T.J., van Duren, L.A., Temmerman, S., Claverie, T., Blanco-Garcia, A., Ysebaert, T., Herman, P.M.J., 2007. Spatial flow and sedimentation patterns within patch of epibenthic structures: combining field, flume and modeling experiments. Continental Shelf Research 27, 1020-1045.

Buijsman, M.C., Ridderinkhof, H., 2007. Long-term ferry-ADCP observations of tidal currents in the Marsdiep inlet. Journal of Sea Research 57, 237–256.

Buijsman, M.C., Ridderinkhof, H., 2008a. Long-term evolution of sandwaves in the Marsdiep inlet. I: high-resolution observations. Continental Shelf Research 28, 1190-1201.

Buijsman, M.C., Ridderinkhof, H., 2008b. Long-term evolution of sandwaves in the Marsdiep inlet. II: Relation to hydrodynamics. Continental Shelf Research 28, 1202– 1215.

Dean R.B., 1974. AERO Report 74-11. Imperial College, London.

Featherstone, R.P., Risk, M.J., 1977. Effect of tube-building polychaetes on intertidal sediments of the Minas Basin, Bay of Fundy. Journal of Sedimentary Petrology 47, 446– 450.

Friedrichs, M., Graf, G., Spring, B., 2000. Skimming flow induced over a simulated polychaete tube lawn at low population densities. Marine Ecology Progress Series 192, 219-228.

Holtmann, S.E., et al., 1996. Atlas of the zoobenthos of the Dutch Continental Shelf. Ministry of Transport, Public Works and Water Management, North Sea Directorate, Rijswijk, 1-244 pp.

Hulscher, S.J.M.H. 1996. Tidal-induced large-scale regular bed form patterns in a three-dimensional shallow water model. Journal of Geophysical Research C9, 101, 20727-20744.

Hulscher, S.J.M.H. and Van den Brink, G.M., 2001, Comparison between predicted and observed sandwaves and sandbanks in the North Sea. Journal of Geophysical Research 106(C5), 9327-9338.

Huthnance, J., 1982, On one mechanism forming linear sandbanks. Estuarine Coastal Shelf Science 14, 79-99.

Morelissen, T., Hulscher, S.J.M.H., Knaapen, M.A.F., Németh, A.A., Bijker, R., 2003. Mathematical modelling of sandwave migration and the interaction with pipelines. Coastal Engineering 48, 197-209.

Németh, A.A., Hulscher, S.J.M.H., de Vriend, H.J., 2003. Offshore sandwave dynamics, engineering problems and future solutions. Pipeline and Gas Journal 230, 67-69.

Németh, A.A., Hulscher, S.J.M.H., van Damme, R.M.J., 2007. Modelling offshore sandwave evolution. Continental Shelf Research 27, 713-728.

O'Donoghue, T., Doucette, J.S., van der Werf, J.J., Ribberink, J.S., 2006. The dimensions of sand ripples in full-scale oscillatory flows. Coastal Engineering 53, 997-1012.

Rabaut, M., Guilini, K., Van Hoey, G., Vincx, M., Degraer, S., 2007. A bio-engineered soft-bottom environment: The impact of Lanice conchilega on the benthic species-specific densities and community structure. Estuarine, Coastal and Shelf Science 75, 525-536.

Roos, P.C. and Hulscher, S.J.M.H., 2003, Large-scale seabed dynamics in offshore morphology: Modeling human intervention, Rev. Geophys., 41(2), 1010.

Soulsby, R. L., 1983. The bottom boundary layer of shelf seas, in Physical Oceanography of Coastal and Shelf Seas, edited by B. Johns, pp. 189–266, Elsevier Sci., New York.

Uittenbogaard, R. 2003. Modelling turbulence in vegetated aquatic flows. In International workshop on RIParian FORest vegetated channels: hydraulic, morphological and ecological aspects, 20-22 February 2003, Trento, Italy, 2003.

Van Dijk, T.A.G.P., Kleinhans, M.G., 2005. Processes controlling the dynamics of compound sandwaves in the North Sea, Netherlands. Journal of Geophysical Research 110. doi 10.1029/2004JF000173.

Van Rijn, L.C., 1991. Sediment transport in combined waves and currents, in Proceedings of Euromech 262, Balkema, A.A., Brookfield, Vt.